

Supporting Information

Directly Insight Into the Formation Driving Force, Sensitivity and Detonation Performance of the Observed CL-20-Based Energetic Cocrystals

Binghui Duan[†], Yuanjie Shu^{†,‡,*}, Ning Liu^{†,‡}, Bozhou Wang^{†,‡}, Xianming Lu^{†,‡},
Yingying Lu[†]

([†]Xi'an Modern Chemistry Research Institute, Xi'an 710065, China;

([‡]State Key Laboratory of Fluorine & Nitrogen Chemicals, Xi'an 710065, China)

Table of contents

Table S1 Crystallographic data for CL-20 and CL-20-based cocrystals

Table S2 Intermolecular hydrogen bonds distances and angles in ϵ -CL-20

Table S3 Intermolecular hydrogen bonds distances and angles in CL-20/DNDAP
cocrystal

Table S4 Intermolecular hydrogen bonds distances and angles in CL-20/DNT
cocrystal

Fig. S1 Hirshfeld surfaces of CL-20 molecules in the crystals

Table S5 Summary of the various intermolecular contact contributions to the CL-20
Hirshfeld surface area in the pure ϵ -CL-20 and CL-20 cocrystals

Table S6 Summary of intermolecular O···O distances in CL-20/DNDAP and
CL-20/MDNT cocrystal

Computational details

Table S7 The interaction energies of the cocrystals

Scheme S1 Isodesmic reactions used to obtain the HOFs of the CL-20 cocrystals and
their components at 298K

Table S8 Experimental gas-phase heats of formation for small molecules at 298 K

Table S9 Detonation properties of pure ϵ -CL-20 and the CL-20 cocrystals

Table S1 Crystallographic data for CL-20 and CL-20-based cocrystals

Crystal	ε -CL-20 ^a	CL-20/DNDAP ^b	CL-20/DNT ^c	CL-20/MDNT ^d
Formula	C ₆ H ₆ N ₁₂ O ₁₂	C ₁₅ H ₂₀ N ₂₈ O ₂₈	C ₂₀ H ₁₈ N ₁₆ O ₂₀	C ₉ H ₉ N ₁₇ O ₁₆
MW/(g/mol)	438.23	1040.59	802.50	611.27
Stoichiometry	—	2:1	1:2	1:1
Space group	<i>P</i> 2 ₁ / <i>n</i>	<i>P</i> 2 ₁ / <i>c</i>	<i>P</i> 1	<i>P</i> 2 ₁ 2 ₁ 2 ₁
<i>a</i> /Å	8.852(2)	13.022(2)	8.145(2)	11.181(6)
<i>b</i> /Å	12.556(3)	22.619(4)	13.612(4)	11.921(7)
<i>c</i> /Å	13.386(3)	12.962(2)	15.415(4)	16.1813(10)
α /deg	90	90	114.692(4)	90
β /deg	106.82(2)	104.648(3)	98.584(5)	90
γ /deg	90	90	93.619(4)	90
Cell vol/Å ³	1424.1(5)	3693.7(12)	1520.3(7)	2156.8(17)
<i>Z</i>	4	4	2	4

^aCited from ref. 1. ^bCited from ref. 2. ^cCited from ref. 3. ^dCited from ref. 4, respectively.

Table S2 Intermolecular hydrogen bonds distances and angles in ε -CL-20¹

Donor-H···A	d(H···A)	<(DHA)/(°)
C(1)-H(1)···O(6)	2.45	136
C(5)-H(5)···O(1)	2.52	150

Table S3 Intermolecular hydrogen bonds distances and angles in CL-20/DNDAP cocrystal²

Donor-H···A	d(H···A)	<(DHA)/(°)
C(8)-H(15)···O(28)	2.45	123
C(7)-H(23)···O(28)	2.48	122
C(15)-H(27C)···O(6)	2.55	142
C(13)-H(25B)···O(1)	2.56	147
C(13)-H(25A)···O(21)	2.58	154
C(15)-H(27A)···O(10)	2.67	137
C(14)-H(26A)···O(3)	2.68	167
C(15)-H(27B)···O(13)	2.68	159
C(6)-H(11)···O(26)	2.72	139

Table S4 Intermolecular hydrogen bonds distances and angles in CL-20/DNT cocrystal³

Donor-H···A	d(H···A)	<(DHA)/(°)
C(1)-H(1A)···O(19)	2.72	144
C(15)-H(15)···O(1)	2.73	116
C(16)-H(16)···O(4)	2.43	135
C(19)-H(19)···O(8)	2.48	168
C(8)-H(8B)···O(9)	2.60	120

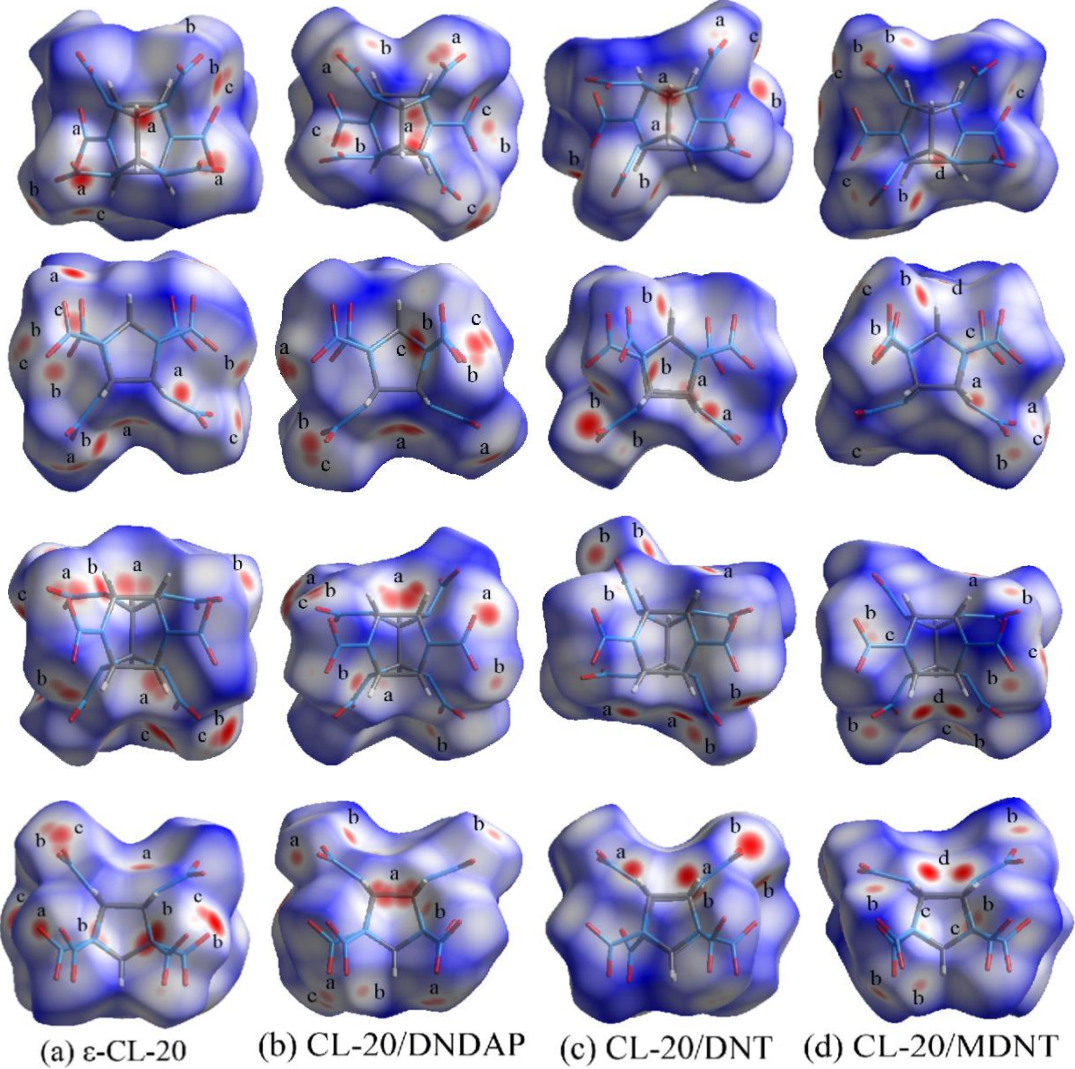


Fig. S1 Hirshfeld surfaces of CL-20 molecules in crystals along different orientations mapped with d_{norm} . a-d denote close contacts of O···H, O···O, O···N and N···H, respectively.

Table S5 Summary of the various intermolecular contact contributions to the CL-20 Hirshfeld surface area in the pure ϵ -CL-20 and CL-20 cocrystals

	ϵ -CL-20	CL-20/DNDAP	CL-20/DNT	CL-20/MDNT
O···O	42.1	36.1	30.2	39.0
O···H	37.0	38.5	50.9	29.8
N···O	18.7	20.7	13.6	21.9
N···H	0.7	0.5	0.6	4.0
N···N	0.1	0.8	0.6	0.3
Others	1.4	3.4	4.1	5.0

Table S6 Summary of intermolecular O···O distances in CL-20/DNDAP and CL-20/MDNT cocrystal. The O···O distances are limited to shorter than 3.3 Å.

Crystal	Atom 1	Atom 2	Length, Å
CL-20/DNDAP cocrystal	O(25)	O(13)	2.987
	O(25)	O(14)	2.950

	O(12)	O(13)	3.265
	O(11)	O(14)	2.929
	O(15)	O(1)	3.091
	O(13)	O(10)	3.089
CL-20/DNT cocrystal	O(2)	O(6)	3.266
	O(1)	O(6)	3.283
	O(3)	O(8)	3.243

Computational details

Intermolecular interaction energy calculation

The intermolecular interaction energies of the CL-20 cocrystals were obtained from calculations of the optimized cocrystal conformation employing Møller-Plesset methods at the MP2/6-311++G(d, p) level⁵ with correction for the basis set superposition error (BSSE) using the Boys-Bernardi counterpoise (CP) technique.⁶ All the calculations were carried out with Gaussian 09.⁷

Table S7. The interaction energies of the cocrystals

	Cocrystal 1	Cocrystal 2	Cocrystal 3
Counterpoise corrected energy/(a.u.)	-2430.51	-2482.14	-2472.30
BSSE energy/(a.u.)	0.0045	0.0004	0.0010
Corrected interaction energy(kJ/mol)	-29.59	-17.51	-3.41

Electrostatic potential (ESP) calculation

Molecular electrostatic potential (ESP), V(r), has been widely used for prediction of nucleophilic and electrophilic sites, as well as molecular recognition mode for a long time, the theoretical basis is that molecules always tend to approach each other in a complementary manner of ESP. ESP can describe the electrostatic distribution in an entire molecule. The electrostatic potentials on the 0.001 a.u. molecular surface are computed by the Multiwfn 3.4 programs⁸ and visualized by VMD programs,⁹ utilizing the B3LYP/6-311++G(d,p) optimized geometries.

Bond dissociation energy (BDE) calculation

Bond dissociation energy (BDE) is defined as the standard enthalpy change of the reaction in which the bond is broken. In general, it is more difficult to detonate a explosive with higher BDE than that with lower BDE. The homolysis equation of bond A–B and its BDE could be expressed as follows:¹⁰



$$BDE = E_A + E_B - E_{A-B}$$

Where A–B is the neutral molecule, A· and B· are the two fragments when the bond

connecting them is broken, respectively. $E_{A\cdot}$, $E_{B\cdot}$, E_{A-B} are the total energies of $A\cdot$, $B\cdot$ and $A-B$, respectively.

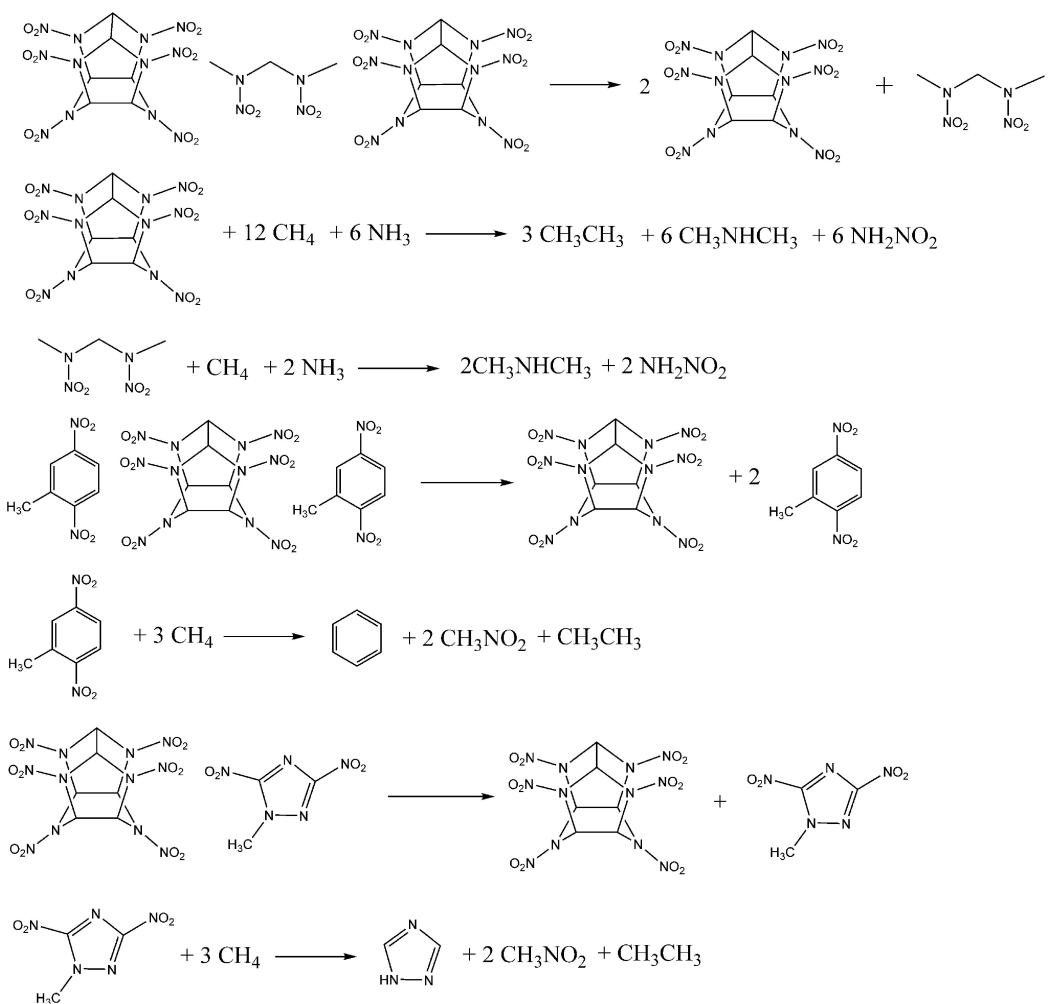
Detonation performance calculation

Detonation velocity (D) and pressure (P) can be estimated using empirical Kamlet-Jacobs equations as follows:¹¹

$$D = 1.01(NM^{1/2}Q^{1/2})^{1/2}(1+1.30\rho)$$

$$P = 1.558\rho^2 NM^{1/2} Q^{1/2}$$

Where D is the detonation velocity (km/s), P is the detonation pressure (GPa), N is the number moles of gaseous products per gram of explosive, M is the average molecular weight of gaseous detonation products, Q is the detonation energy (cal/g) and ρ is crystal density (g/cm³). The isodesmic reactions used for the prediction of gas-phase heats of formation (HOFs) are shown in Scheme S1 and the experimental HOFs of the small molecules used in the isodesmic reactions are listed in Table S6.



Scheme S1 The isodesmic reactions used for the prediction of gas-phase heats of formation

(HOFs) at 298 K

Table S8 Experimental gas-phase heats of formation for small molecules at 298 K¹²⁻¹⁴

Compounds	$\Delta H_{f,gas}/(\text{kJ/mol})$
CH ₄	-74.6
NH ₃	-46.1
CH ₃ CH ₃	-84.0
CH ₃ NHCH ₃	-18.8
NH ₂ NO ₂	-3.9
1H-1,2,4-triazole	193.70
benzene	82.89

Table S9 Detonation properties of pure ϵ -CL-20 and the CL-20 cocrystals

	HOF(kJ/mol)	$\rho/(\text{g/cm}^3)$	$D/(\text{m/s})$	P/GPa
ϵ -CL-20	430.5	2.04	9666	45.4
Cocrystal 1	614.2	1.87	8958	37.1
Cocrystal 2	560.7	1.75	7880	27.6
Cocrystal 3	726.5	1.88	9055	38.3

References

- 1 X. Q. Zhao and N. C. Shi, *Chin. Sci. Bull.*, 1995, **40**, 2158-2160.
- 2 N. Liu, B. H. Duan, X. M. Lu, H. C. Mo, M. H. Xu, Q. Zhang and B. Z. Wang, *CrystEngComm*, 2018, **20**, 2060-2067.
- 3 K. Liu, G. Zhang, J. Luan, Z. Chen, P. Su and Y. Shu, *J. Mol. Struct.*, 2016, **1110**, 91-96.
- 4 S. R. Anderson, P. Dubé, M. Krawiec, J. S. Salan, D. J. Am Ende and P. Samuels, *Propellants, Explos., Pyrotech.*, 2016, **41**, 783-788.
- 5 Y. Zhao and D. G. Truhlar, *Acc. Chem. Res.*, 2008, **41**, 157-167.
- 6 S. F. Boys and F. Bernardi, *Mol. Phys.* 1970, **19**, 553.
- 7 M. J. Frisch, G. W. Trucks, H. B. Schlegel, G. E. Scuseria, M. A. Robb, J. R. Cheeseman, G. Scalmani, V. Barone, B. Mennucci, G. A. Petersson, H. Nakatsuji, M. Caricato, X. Li, H. P. Hratchian, A. F. Izmaylov, J. Bloino, G. Zheng, J. L. Sonnenberg, M. Hada, M. Ehara, K. Toyota, R. Fukuda, J. Hasegawa, M. Ishida, T. Nakajima, Y. Honda, O. Kitao, H. Nakai, T. Vreven, J. A. Montgomery, Jr., J. E. Peralta, F. Ogliaro, M. Bearpark, J. J. Heyd, E. Brothers, K. N. Kudin, V. N. Staroverov, R. Kobayashi, J. Normand, K. Raghavachari, A., Rendell, J. C. B., S. S. Iyengar, J. Tomasi, M. Cossi, N. Rega, J. M. Millam, M. Klene, J. E. Knox, J. B. Cross, V. Bakken, C. Adamo, J. Jaramillo, R. Gomperts, R. E. Stratmann, O.

- Yazyev, A. J. Austin, R. Cammi, C. Pomelli, J. W. Ochterski, R. L. Martin, K. Morokuma, V. G. Zakrzewski, G. A. Voth, P. Salvador, J. J. Dannenberg, S. Dapprich, A. D. Daniels, Ö. Farkas, J. B. Foresman, J. V. Ortiz, J. Cioslowski, Fox, D. J., Gaussian 09, Revision D.01. Gaussian, Inc., Wallingford CT, 2013.
- 8 T. Lu and F. Chen, *J. Mol. Graph. Model.*, 2012, **38**, 314-323.
- 9 W. Humphrey, A. Dalke and K. Schulten, *J. Mol. Graphics*, 1996, **14**, 33-38.
- 10 P. Y. Chen, L. Zhang, S. G. Zhu and G. B. Cheng, *Can. J. Chem.* 2015, **93**, 632-638.
- 11 M. J. Kamlet, S. J. Jacobs, *J. Chem. Phys.*, 1968, **48**, 23-35.
- 12 D. R. Lide, Handbook of Chemistry and Physics (Section 5). 84 ed.; CRC Press: Boca Raton: pp 2003-2004.
- 13 J. P. McCullough, D. W. Scott, R. E. Pennington, I. A. Hossenlopp and G. Waddington, *J. Am. Chem. Soc.*, 1954, **76**, 175-186.
- 14 P. Jimenez, M. V. Roux and C. Turrian, *J. Chem. Thermodyn.* 1989, **21**, 759-764.